

# Virtual four-dimensional imaging of lung parenchyma by optical coherence tomography in mice

## Sven Meissner

University of Technology Dresden  
Clinical Sensing and Monitoring  
Medical Faculty  
Fetscherstrasse 74  
01307 Dresden, Germany

## Arata Tabuchi

St. Michael's Hospital  
30 Bond Street  
Toronto, M5B 1W8 Ontario, Canada

## Michael Mertens

Charité-Universitätsmedizin Berlin  
Department of Physiology  
Arnimallee 22  
14195, Berlin, Germany

## Wolfgang M. Kuebler

St. Michael's Hospital  
30 Bond Street  
Toronto, M5B 1W8 Ontario, Canada  
and  
Charité-Universitätsmedizin Berlin  
Department of Physiology  
Arnimallee 22  
14195, Berlin, Germany

## Edmund Koch

University of Technology Dresden  
Clinical Sensing and Monitoring  
Medical Faculty  
Fetscherstrasse 74  
01307 Dresden, Germany

## 1 Introduction

The development of protective ventilation strategies to improve mechanical ventilation of patients in intensive care is of great importance. In particular, the ventilation of acute respiratory distress syndrome (ARDS) patients has to be improved to decrease the mortality of patients with lung injuries. Furthermore, artificial ventilation has to be optimized to prevent worsening of pre-existing lung injuries.<sup>1-3</sup> However, approaches to improve artificial ventilation are hampered by our lack of understanding of their effects on the actual units of gas exchange, i.e., the alveoli. One approach to circumvent this limitation is the development of numerical models of the lung on an alveolar scale.<sup>4</sup> With the help of such models, alveolar dynamics can be simulated and different protective ventilation strategies can be characterized concerning the mechanical

**Abstract.** In this feasibility study, we present a method for virtual 4-D imaging of healthy and injured subpleural lung tissue in the ventilated mouse. We use triggered swept source optical coherence tomography (OCT) with an A-scan frequency of 20 kHz to image murine subpleural alveoli during the inspiratory phase. The data acquisition is gated to the ventilation pressure to take single B-scans in each respiration cycle for different pressure levels. The acquired B-scans are combined off-line into one volume scan for each pressure level. The air fraction in healthy lungs and injured lungs is measured using 2-D OCT en-face images. Upon lung inspiration from 2 to 12 cmH<sub>2</sub>O ventilation pressure, the air fraction increases in healthy lungs by up to 11% and in injured lungs by 8%. This expansion correlates well with results of previous studies, reporting increased alveolar area with increased ventilation pressures. We demonstrate that OCT is a useful tool to investigate alveolar dynamics in spatial dimensions. © 2010 Society of Photo-Optical Instrumentation Engineers. [DOI: 10.1117/1.3425654]

Keywords: optical coherence tomography; lung injury; alveolar dynamics; alveolar geometry; alveolar mechanics.

Paper 10130LR received Mar. 17, 2010; revised manuscript received Apr. 9, 2010; accepted for publication Apr. 9, 2010; published online May 20, 2010.

stress exerted on the alveolar structures. The basis for such models is detailed knowledge of the alveolar behavior in an *in vivo* situation, especially information about alveolar volume change during the breathing cycle. However, adequate *in vivo* 3-D information about the parenchymal dynamics at the level of individual alveoli is not available in the current literature. The most established modality to image *in vivo* lung tissue at the alveolar level is intravital microscopy (IVM), which allows 2-D, high resolution, and real-time imaging of the subpleural lung surface. Yet IVM does not provide 3-D information on alveolar dynamics during ventilation.<sup>5</sup> Additionally, there are focusing problems during the ventilation cycle for this technique, requiring the positioning of cover glasses on the lung surface for stabilization, which in turn may influence the dynamic behavior of the imaged alveoli beneath. 3-D imaging techniques like computed tomography or magnetic resonance tomography, on the other hand, do not provide a sufficient spatial resolution to image alveoli *in vivo*.<sup>6,7</sup> To investigate the

Address all correspondence to: Sven Meissner, University of Technology Dresden, Clinical Sensing and Monitoring, Medical Faculty, Fetscherstrasse 74, 01307 Dresden, Germany. Tel: 49-351-458-6133; Fax: 49-351-458-6325; E-mail: sven.meissner@tu-dresden.de.

alveolar behavior during ventilation *in vivo*, an imaging technique is hence required that provides high resolution, allows for 3-D imaging without influencing the alveolar mechanics, yields high acquisition rates to perform real-time imaging, and can be applied *in vivo*. Optical coherence tomography (OCT)<sup>8</sup> is an optical imaging technique allowing contactless 3-D imaging of strongly scattering samples like biological tissue. With a spatial resolution of less than 10  $\mu\text{m}$  and measurement ranges of up to 2 mm, OCT is suitable to image subpleural alveoli that have diameters of approximately 100  $\mu\text{m}$ .<sup>9</sup>

## 2 Methods and Materials

### 2.1 Animal Model

All experiments were performed in accordance with the *Guide for the Care and Use of Laboratory Animals* (Institute of Laboratory Animal Resources, 7th edition, 1996). The study was approved by the animal care and use committee of the local government authorities. In anesthetized mice ( $n=5$ ), a thorax window was surgically prepared as described in detail by Tabuchi, Pries, and Kuebler.<sup>10</sup> The window was closed by a transparent membrane, and negative intrapleural pressure was reconstituted via a transdiaphragmal catheter. The prepared window is suitable to perform *in vivo* imaging of subpleural alveoli by 3-D optical coherence tomography (OCT). The mice were mechanically ventilated with room air at a frequency of 100 breaths per minute, an inspiratory plateau pressure of 12  $\text{cmH}_2\text{O}$ , and a positive end expiratory pressure of 2  $\text{cmH}_2\text{O}$ . Arterial blood pressure was continuously measured as a vital parameter by an intra-arterial catheter in the carotis artery. Lung injury was induced by endotracheal application of hydrochloric acid ( $\text{pH}=1.5$ ; 2  $\mu\text{l/g}$  body weight).

### 2.2 Image Acquisition

A swept source OCT system with an axial and lateral resolution of 12  $\mu\text{m}$  in air was used. The used light source is centered at 1320 nm and provides a 100-nm-wide spectrum [full-width at half maximum (FWHM)], an optical power of approximately 15 mW, and a tuning rate of 20 kHz. *In vivo* 3-D OCT imaging of murine subpleural alveoli gated to the inspiratory and expiratory plateau phases in healthy as well as injured mouse lungs has previously been reported by us.<sup>11</sup> Due to the improvement of the data acquisition speed of the OCT technique, it is now no longer necessary to gate the OCT imaging to the plateau phases. The 20-kHz line rate of the used OCT system facilitates the acquisition of 3-D OCT image stacks in the inspiratory phase. The data acquisition is triggered to the pulmonary airway pressure measured on-line by the ventilator. To acquire 3-D image stacks at different pressure levels during the inspiratory phase, the acquisition of the image stack was divided into the acquisition of single B-scans. In every respiratory cycle, one B-scan was acquired at a defined airway pressure. The single B-scans were assembled off-line to one 3-D OCT image stack for each pressure level during the inspiratory phase. 3-D OCT image stacks were obtained at airway pressures of 2/3/4/5/6/7/8/9/10, and 11  $\text{cmH}_2\text{O}$  to document the dynamic changes of subpleural alveolar structures during the inspiratory phase by time-resolved 3-D OCT datasets. We call this images stack “virtual

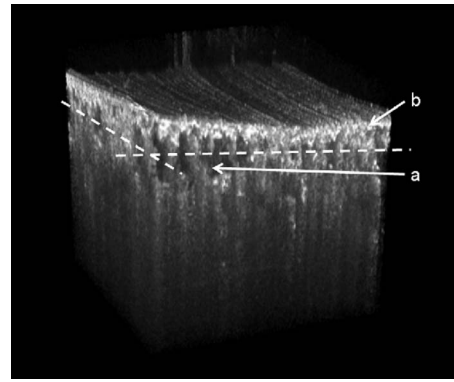


**Fig. 1** A volume rendering of subpleural alveolar tissue. The tissue block has dimensions of  $1500 \times 1500 \times 1500 \mu\text{m}^3$ . The visceral pleura (part b) and single alveoli (part a) can be detected. The dashed line shows the cutting plane, which was used to extract the en-face images for alveolar area quantification. The shift between single B-scans is attributable to motion artifacts caused by the heartbeat.

4-D” because we acquire 3-D images of the lung parenchyma with temporal resolution during the inspiratory phase. The acquired datasets have a dimension of  $192 \times 192 \times 512$  pixels, which corresponds to a volume ( $x/y/z$ ) of  $1.5 \times 1.5 \times 3 \text{ mm}^3$ . The identical area was imaged again 2 h after instillation of hydrochloric acid to assess the changes of alveolar dynamics in the acutely injured lung.

### 2.3 Image Analysis

En-face OCT images were taken from the 3-D OCT datasets to quantify the alveolar area change during the inspiration phase. The procedure of extracting the OCT en-face images is described in detail in Meissner et al.<sup>12,13</sup> The extracted 2-D images display the subpleural alveolar tissue at a depth of approximately 45  $\mu\text{m}$  beneath and parallel to the pleura. In these images, all alveolar areas not touching the image border were quantified and normalized to the respective area measured at an airway pressure of 2  $\text{cmH}_2\text{O}$ .<sup>12,13</sup>

## 3 Results

Evaluation of the acquired image stack demonstrates that virtual 4-D, airway pressure-gated imaging of subpleural lung tissue *in vivo* is in principle feasible by OCT. Figure 1 presents an exemplarily volume rendering taken from an injured lung at an airway pressure of 8  $\text{cmH}_2\text{O}$ . The lung tissue is bordered by the visceral pleura (part b), which can be seen on the upper side of the tissue block. Furthermore, single alveoli (part a) are recognizable beneath the pleura. The dashed line represents the plane that was used to extract the OCT en-face images for analysis at a depth of approximately 45  $\mu\text{m}$  beneath the pleura. The picture series shown in Fig. 2 displays the OCT en-face images taken from the 3-D datasets. In the upper two rows are images of healthy lung tissue, and in the lower rows are images of injured lung tissue from the same animal. The image sequences show alveolar changes with increasing airway pressures during the inspiratory phase. Black structures in the en-face images represent the air-filled alveoli, and white structures are the alveolar walls. Identical structures can be observed in all images, demonstrated by the landmark

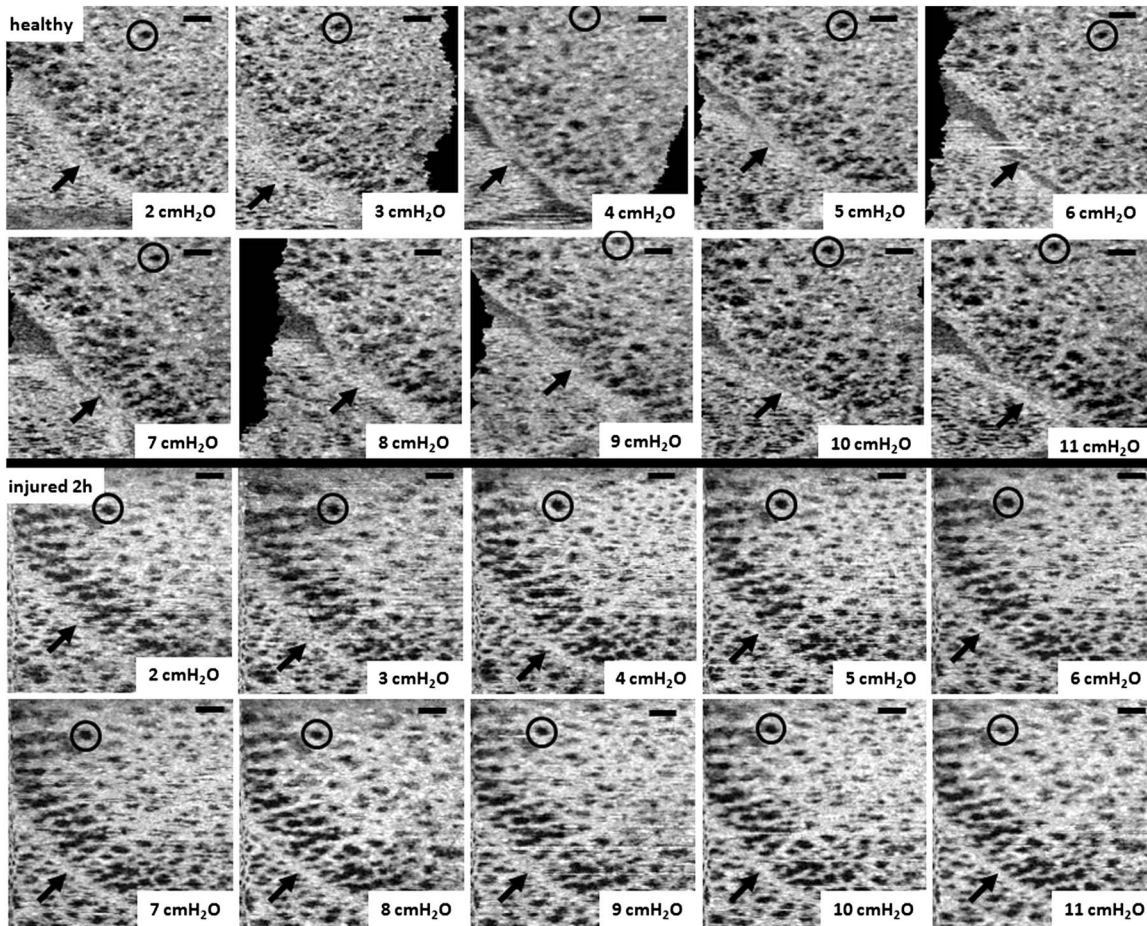


**Fig. 2** Image sequences showing OCT en-face images of healthy (upper rows) and injured (lower rows) lung of the same animal. The images were extracted from the 3-D OCT image stacks acquired during the inspiratory phase from 2 to 11 cmH<sub>2</sub>O. An alveolar landmark is highlighted in all images by the black circle. The black arrow denotes the margin between two lung lobes. A large dislocation of this margin can be recognized with increasing airway pressures in the healthy lung, in contrast to the injured lung, where the location of the interlobar margin remains unchanged, suggesting that alveolar expansion is decreased. Scale bar is 200  $\mu$ m.

in the OCT en-face images. However, in the image taken at 8 cmH<sub>2</sub>O airway pressure in the healthy lung, it was impossible to identify this structure. Furthermore, the margin between two lung lobes is recognizable and denoted by the black arrow. The main difference between the image sequences obtained in healthy and injured lungs is the reduced movement of the injured lung during the inspiratory phase, as demonstrated by the lack of dislocation of the lobe margin. This notion is supported by the quantitative analysis of alveolar distension in healthy and injured lungs. Figure 3 shows the alveolar area change during the increase of airway pressure from 2 to 11 cmH<sub>2</sub>O in the inspiratory phase. Alveolar area was normalized to the area measured at 2 cmH<sub>2</sub>O. The black line presents the area change in an exemplarily healthy lung, the dashed line in an injured lung. Both graphs show an increase in alveolar area with increasing airway pressure during the inspiratory phase. In healthy lungs, the major part of expansion occurs between 2 and 4 cmH<sub>2</sub>O airway pressure, whereas the larger part of expansion in injured lungs happens at airway pressures higher than 8 cmH<sub>2</sub>O. Compared to alveolar size at 2 cmH<sub>2</sub>O, the increase of airway pressure to 11 cmH<sub>2</sub>O increased alveolar area in healthy lungs by 12%,

while alveoli only expanded by 8% in injured lungs. Both the right shift of the area-pressure curve and the overall reduced alveolar expansion reflect the reduced alveolar compliance and the increased stiffness of the injured lung.

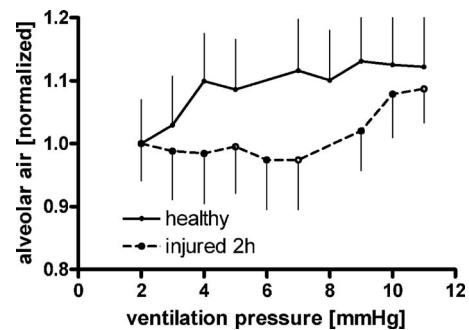


**Fig. 3** Line graph showing exemplarily pressure-dependent changes in alveolar area during the inspiratory phase normalized to the area at 2 cmH<sub>2</sub>O for a healthy (solid) and after induced lung injury (dashed).



## 4 Discussion

In this study, we demonstrate the feasibility of *in vivo* virtual 4-D imaging of subpleural alveolar structures by optical coherence tomography in healthy and injured lungs of ventilated mice. This new method allows for imaging of alveoli during the dynamic respiratory cycle without applying constant positive airway pressure (CPAP)<sup>12</sup> or gating to the inspiratory or expiratory plateau phases.<sup>11</sup> During the entire data acquisition process, the mouse is regularly ventilated, warranting that the recorded data realistically reflect the physiological situation in the dynamically ventilated lung. Off-line assembly of the single B-scans acquired in sequent respiratory cycles at different pressure levels allows for virtual 4-D imaging of the lung parenchyma. We termed the acquired image stacks virtual 4-D, since the reconstructed 3-D image stacks at different airway pressures in fact represent the tissue at the identical phase of the ventilation cycle, because the acquisition of each stack was carried out over a series of successive breathing cycles. The observed expansion of the alveolar area in healthy lungs and the reduced alveolar compliance in lung injury corresponds to our previously reported data from OCT and IVM imaging *in vivo*<sup>11</sup> and in isolated lungs.<sup>9</sup> Our results are thus in accordance with the notion of decreased alveolar expansion in lung injury due to stiffening of the lung parenchyma.<sup>12</sup> However, the alveolar expansion measured in this study is smaller than comparable data on alveolar expansion published previously.<sup>11,12</sup> This quantitative discrepancy is likely attributable in part to different experimental conditions. In our study, fast data acquisition during the regular inspiratory phase allowed us to refrain from the application of CPAPs over a longer period of time, like in studies with isolated lungs.

Taken together, the presented imaging technique allows to our knowledge the first virtual 4-D imaging of subpleural alveoli *in vivo*. The method can be further improved by using faster and higher spatially resolving OCT setups to obtain more detailed knowledge about the alveolar dynamics during the ventilation cycle.<sup>14,15</sup> A faster OCT system will also allow minimizing motion artifacts, while high resolution setups can reduce the apparent underestimation of the alveolar area by the OCT technique.<sup>12</sup>

### Acknowledgments

This project was supported by the German Research Foundation (DFG) "Protective Artificial Respiration" (PAR)—KO 1814/6-1 and KU 1218/4-1.

## References

1. J. A. Frank and M. A. Matthay, "Science review: mechanisms of ventilator-induced injury," *Crit. Care* **7**, 233–241 (2003).
2. K. F. Udobi, E. Childs, and K. Touijer, "Acute respiratory distress syndrome," *Am. Fam. Physician* **67**, 315–322 (2003).
3. D. Carney, J. DiRocco, and G. Nieman, "Dynamic alveolar mechanics and ventilator-induced lung injury," *Crit. Care Med.* **33**, 122–S128 (2005).
4. H. Kitaoka, G. F. Nieman, Y. Fujino, D. Carney, J. DiRocco, and I. Kawase, "A 4-dimensional model of the alveolar structure," *J. Physiol. Sci.* **57**, 175–185 (2007).
5. H. J. Schiller, U. G. McCann, D. E. Carney, L. A. Gatto, J. M. Steinberg, and G. F. Nieman, "Altered alveolar mechanics in the acutely injured lung," *Crit. Care Med.* **29**, 1049–1055 (2001).
6. M. Gama de Abreu, M. Cuevas, P. M. Spieth, A. R. Carvalho, V. Hietschold, C. Stroszczyński, B. Wiedemann, T. Koch, P. Pelosi, and E. Koch, "Regional lung aeration and ventilation during pressure support and biphasic positive airway pressure ventilation in experimental lung injury," *Crit. Care* **14**(2), R34 (2010).
7. E. van Beek, J. M. Wild, H. U. Kauczor, W. Schreiber, J. P. Mugler, and E. E. de Lange, "Functional MRI of the lung using hyperpolarized 3-helium gas," *J. Magn. Reson. Imaging* **20**, 540–554 (2004).
8. D. Huang, E. A. Swanson, C. P. Lin, J. S. Schuman, W. G. Stinson, W. Chang, M. R. Hee, T. Flotte, K. Gregory, C. A. Puliafito, and J. G. Fujimoto, "Optical coherence tomography," *Science* **254**, 1178–1181 (1991).
9. A. Popp, M. Wendel, L. Knels, T. Koch, and E. Koch, "Imaging of the three-dimensional alveolar structure and the alveolar mechanics of a ventilated and perfused isolated rabbit lung with Fourier transform optical coherence tomography," *J. Biomed. Opt.* **11**(1), 14015 (2006).
10. A. Tabuchi, A. R. Pries, W. M. Kuebler, "A new model for intravital microscopy of the murine pulmonary microcirculation," *FASEB J.* **20**, A285–A286 (2006).
11. M. Mertens, A. Tabuchi, S. Meissner, A. Krueger, U. Kertzscher, A. R. Pries, K. Affeld, A. S. Slutsky, E. Koch, and W. M. Kuebler, "Alveolar dynamics in acute lung injury: heterogeneous distension rather than cyclic recruitment," *Crit. Care Med.* **37**(9), 2604–2611 (2009).
12. S. Meissner, L. Knels, A. Krüger, T. Koch, and E. Koch, "Simultaneous 3D optical coherence tomography and intravital microscopy for imaging subpleural pulmonary alveoli in isolated rabbit lungs," *J. Biomed. Opt.* **14**(5), 054020 (2009).
13. S. Meissner, L. Knels, and E. Koch, "Improved 3D Fourier domain optical coherence tomography by index matching in alveolar structures," *J. Biomed. Opt.* **14**(6), 064037 (2009).
14. R. Huber, D. C. Adler, V. J. Srinivasan, and J. G. Fujimoto, "Fourier domain mode locking at 1050 nm for ultra-high-speed optical coherence tomography of the human retina at 236,000 axial scans per second," *Opt. Lett.* **32**, 2049–2051 (2007).
15. P. Cimalla, J. Walther, M. Mehner, M. Cuevas, and E. Koch, "Simultaneous dual-band optical coherence tomography in the spectral domain for high resolution *in vivo* imaging," *Opt. Express* **17**(22), 19486–19500 (2009).